EMBO Molecular Medicine

Rab25 increases cellular ATP and glycogen stores protecting cancer cells from bioenergetic stress

Kwai Wa Cheng[1,†], Roshan Agarwal[1,2†], Shreya Mitra[1], Ju-Seog Lee[1], Mark Carey[1,3], Joe W. Gray[4], Gordon B. Mills[1]*

Keywords: AKT; bioenergetic; cell death; glycogen; Rab25

DOI 10.1002/emmm.201100193

Received September 20, 2010
Revised November 29, 2011
Accepted November 30, 2011

Cancer cells are metabolically stressed during tumour progression due to limited tumour vascularity and resultant nutrient, growth factor and oxygen deficiency that can induce cell death and inhibit tumour growth. We demonstrate that Rab25, a small GTPase involved in endosomal recycling, that is genomically amplified in multiple tumour lineages, is a key regulator of cellular bioenergetics and autophagy. *RAB25* enhanced survival during nutrient stress by preventing apoptosis and autophagy via binding and activating AKT leading to increased glucose uptake and improved cellular bioenergetics. Unexpectedly, Rab25 induced the accumulation of glycogen in epithelial cancer cells, a process not previously identified. Strikingly, an increase in basal ATP levels combined with AKT-dependent increases in glucose uptake and glycogen storage allowed maintenance of ATP levels during bioenergetic stress. The clinical relevance of these findings was validated by the ability of a Rab25-dependent expression profile enriched for bioenergetics targets to identify patients with a poor prognosis. Thus, Rab25 is an unexpected regulator of cellular bioenergetics implicated as a useful biomarker and potential therapeutic target.

INTRODUCTION

Cancer cells characteristically require higher levels of nutrients and energy metabolism than normal cells, due to increased rates of cell proliferation that demand synthesis of proteins, lipids and nucleotides as well as energy in the form of adenosine 5′-triphosphate (ATP; Vander Heiden et al, 2009). However, as cancers grow and metastasize, they frequently outpace their vascular supply resulting in both nutrient and oxygen deprivation. ATP, the main cellular energy source, is produced primarily from two sources, glycolysis and mitochondrial respiration (Krebs cycle and oxidative phosphorylation), with oxidative phosphorylation providing the majority of ATP. Cancer cells, with respect to their normal counterparts, demonstrate increased glycolytic capacity even in the presence of adequate oxygen supplies (Moreno-Sánchez et al, 2007) providing energy as well as increased production of cellular building blocks such as amino acids and fatty acids (Vander Heiden et al, 2009).

RAB GTPases comprise the largest subfamily of small GTPases and play a master role in regulating intercellular vesicle transport and trafficking of proteins (Agarwal et al, 2009). Numerous studies have implicated aberrations in Rab-regulated vesicle recycling in the initiation and progression of multiple cancer lineages (Mosesson et al, 2008). We have previously shown that RAB25 is a candidate oncogene located within the 1q22 amplicon in ovarian and breast cancers (Cheng et al, 2004). Rab25, which is primarily expressed in epithelial cells (Goldenring et al, 1993), is a member of the Rab11 subfamily with its closest homologues Rab11a and Rab11b (Agarwal et al, 2009). Functional studies demonstrate that the

(1) Department of Systems Biology, University of Texas MD Anderson Cancer Center, Houston, TX, USA
(2) Current address: Department of Surgery and Cancer, Imperial College London, London, UK
(3) Current address: Department of Obstetrics & Gynaecology, University of British Columbia, Vancouver, Canada
(4) Lawrence Berkley National Laboratory, Berkeley, CA, USA
***Corresponding author:** Tel: +1 713 834 6159; Fax: +1 713 5634235; E-mail: kwcheng@mdanderson.org

†These authors contributed equally to this work.

Rab11 subfamily is involved in transcytosis, endocytic sorting and transport across polarized epithelial cells as well as in apical vesicle recycling (Tzaban et al, 2009).

RAB25 is amplified and over-expressed in many human cancers. Increased RAB25 mRNA levels have been reported in ovarian, prostate cancer, transitional cell carcinoma of the bladder, invasive breast cancer, liver cancer and Wilms tumour (Agarwal et al, 2009), suggesting a pathological role of Rab25 in development or progression of multiple tumour lineages. In addition, we and others have demonstrated that Rab25 increases anchorage-independent growth, survival in response to growth factor deprivation, suppresses apoptosis and increases tumour development, while down-regulation of Rab25 by RNAi transfection significantly inhibits ovarian cancer growth *in vivo* (Cheng et al, 2004; Fan et al, 2006). Recent studies demonstrated that expression of Rab25 in rat intestine epithelial cells leads to transformation and cancer development (Lapierre et al, 2011). Further, Rab25 genomic amplification and increased mRNA expression are both associated with poor prognosis in a subset of ovarian and breast cancers (Cheng et al, 2004). Together, these data strongly implicate Rab25 in tumour initiation and aggressiveness. However, Rab25 has also been suggested to act as a tumour suppressor in claudin-low breast cancers and in bowel epithelium (Cheng et al, 2010; Nam et al, 2010). Thus, Rab25 may function as an oncogene or a tumour suppressor depending on the cellular context and the extracellular environment of the tumour.

Analysis of transcriptional profiles has emerged as a powerful tool in elucidating the molecular mechanisms by which a genetic aberration contributes to cancer development (Nevins & Potti, 2007). To explore the mechanisms by which Rab25 expression alters cancer cell function, we identified a *RAB25* transcriptome *in vitro*. Importantly, the Rab25 signature is portable from cell lines allowing interrogation of tumour samples. The transcriptome was highly enriched in genes implicated in cellular metabolism indicating a novel role of Rab25 in regulating cellular metabolism that we explore further herein.

RESULTS

The Rab25 transcriptome is enriched in metabolism-associated genes leading to decreased cellular sensitivity to nutrient stress

Transcriptional profiling revealed a Rab25-dependent gene expression signature containing 1128 probes representing 908 known genes [Fig S1A–C and Table S1 of Supporting information, raw data was submitted to Gene ExpressionOmnibus (GSE28299)]. Based on GeneOntology Biological Process Classification, metabolism-associated genes constituted the largest category, with over 47% of the Rab25-dependent gene expression signature being implicated in cellular metabolism, including lipid, amino acid and carbohydrate metabolism (Fig S1D and Table S2 of Supporting information). Based on this potential novel role for Rab25 in regulating cellular metabolism and the increased glycolytic dependence of cancer cells, it was of particular interest to evaluate whether Rab25 alters cell survival during nutrient stress by culturing cells under glucose (deprivation or by addition of 2-deoxyglucose; 2DG) or amino acid (EBSS) deprivation conditions. As growth factors are required for efficient uptake and utilization of nutrients (Edinger & Thompson, 2002), growth factor deprivation provides a potent mimic of decreased cellular energy balance and increased cellular stress.

Expression of *RAB25* (to levels present in tumours with amplified *RAB25*) in ovarian cancer A2780 and HEY cells or IOSE29ht immortalized normal ovarian epithelium cells, all of which express low endogenous levels of *RAB25*, significantly decreased cell death ($p < 0.01$) under growth factor and nutrient deprivation conditions, as measured by DNA fragmentation and flow cytometry of fluorescent-tagged deoxyuridine triphosphate nucleotide incorporation (Fig 1A and B). In contrast, decreasing Rab25 expression with siRNA sensitized cells to nutrient withdrawal-induced cell death (Fig 1B). To further evaluate the physiological relevance of these findings, we examined the

Figure 1. Rab25 expression alters cells sensitivity to nutrient stress.

A. Rab25 expression decreases nutrient withdrawal (24 h) induced cell death in ovarian A2780 and IOSE29 cells measured using the Cell death ELISA plus assay (left); cells were cultured in complete media (containing 5% FBS), serum free media (SF), complete media plus 2DG, serum and glucose free media (SF-glu), or in amino acid, glucose and SF Earls buffer salt solution (EBSS). (a) $p < 0.01$ *versus* control and (b) $p < 0.05$ *versus* pcDNA. (Right) Percentage of apoptotic cells (sub-G_0 population) by flow cytometry in A2780 cells following glucose and serum withdrawal (Glu/SF). (a) $p < 0.001$ *versus* A2780 pcDNA control and (b) $p < 0.05$ A2780 Rab25 *versus* A2780 pcDNA control.

B. Decreasing Rab25 expression increases sensitivity to nutrient stress induced cell death. Expression of Rab25 was down-regulated by siRNA or shRNA specific to Rab25.

C. Rab25 regulates autophagy activity in ovarian cancer cells under serum and glucose deprivation conditions. Western blot for the 16kD LC3-II fragment, indicative of autophagy activity, in A2780 cells after 4 and 6 h of serum and glucose withdrawal.

D. Electron microscopic analysis of autophagy in ovarian A2780 cells after 4 and 24 h of serum and glucose withdrawal (upper panel, low magnification). High magnification images of boxed areas with arrowheads depicting autophagic vacuoles (lower panel, inset; N: nucleus). Average number of autophagosomes per cell was calculated by counting the number of autophagosomes in 16 individual cells from two-independent experiments.

E-H. Expression of Rab25 decreases glucose and serum deprivation induced signalling activation. Protein expression was measured by RPPA or WB analysis.

E. RPPA detection of time-dependent activation of AMPK after nutrient withdrawal.

F. WB analysis of AMPK and acetyl-CoA carboxylase (ACC) phosphorylation in HEY ovarian cancer cells (upper panel). WB of phospho-ACC levels in A2780, IOSE80ht and SKOV3 ovarian cells after 1 h of nutrient withdrawal (lower panel).

G. RPPA detection of phosphorylation of ACC after withdrawal of serum and glucose.

H. Effect of Rab25 down-regulation on AMPK (left panel) and ACC (right panel) phosphorylation. Total cellular protein, isolated from A2780 pcDNA and Rab25 expressing cells 72 h post-transfection with either non-target (NT) RNAi or Rab25 specific RNAi, was separated by polyacrylamide gel electrophoresis (PAGE) followed by WB analysis. (a) $p < 0.001$ *versus* NT RNAi control and (b) $p < 0.001$, pcDNA *versus* Rab25.

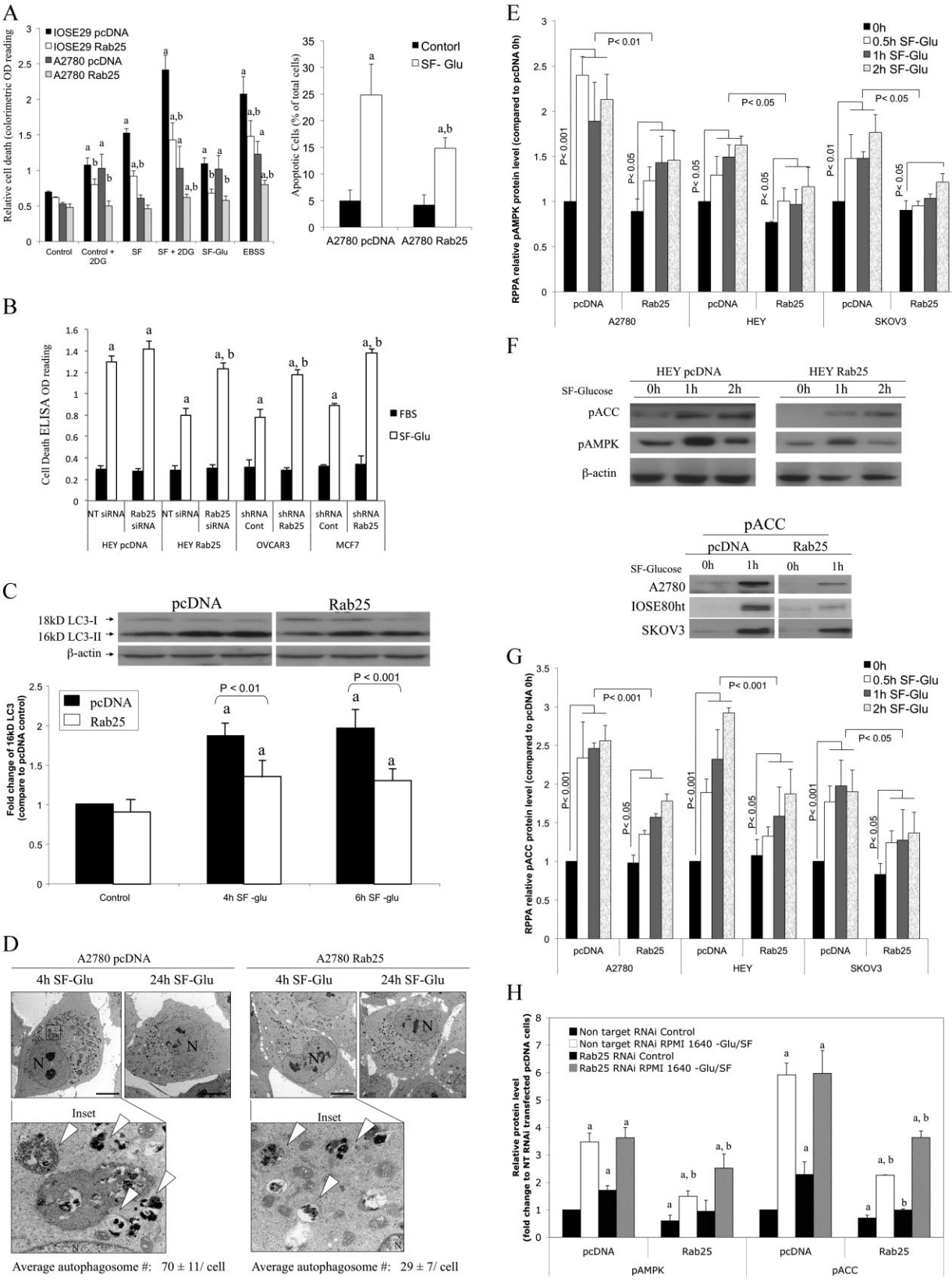

Figure 1.

effect of decreasing Rab25 expression in ovarian OVCAR3 and breast MCF7 cancer cell lines, which express high endogenous Rab25 levels (Cheng et al, 2005). Stable expression of shRNA specific to Rab25 significantly reduced the expression of Rab25 protein in these cells (Fig S2 of Supporting information). Similar to the results obtained from HEY cells, reducing Rab25 expression by shRNA led to increased cell death after nutrient withdrawal in both OVCAR3 and MCF7 cells (Fig 1B).

Under conditions of reduced nutrient availability most cells undergo autophagy, degrading cytoplasmic organelles to provide substrates for energy metabolism (Meijer & Codogno, 2004). To elucidate the contribution of autophagy to Rab25-mediated resistance to metabolic stress in cancer cells, the formation of autophagosomes, the final step in the autophagy cascade, was assessed by measuring the levels of the endogenous autophagosomal marker LC3, microtubule-associated protein1 light chain 3, by Western blotting (WB) after 4 and 6 h of nutrient withdrawal (Mizushima, 2004). Surprisingly, LC3-II protein fragment levels were lower in Rab25-expressing A2780 and HEY cells than in control pcDNA-transfected cells after serum and glucose withdrawal (Fig 1C), suggesting a change in autophagic activity. Consistent with the WB data, expression of Rab25 markedly decreased autophagosome formation (Fig 1D) in Rab25-expressing A2780 cells (29 ± 7 autophagosome/cells) compared to control cells (70 ± 11 autophagosomes/cells) after both glucose and serum withdrawal for 4 h ($p < 0.00057$) as assayed by electron microscopy (EM), a quantitative and definitive method for detection of autophagy (Mizushima, 2004). However, prolonged nutrient withdrawal (24 h) was sufficient to induce autophagy in Rab25-transfected cells to levels similar to those in parental cells, indicating that the autophagic machinery is not compromised by the expression of Rab25 but rather that autophagy induction is delayed.

The Rab25-mediated reduction in autophagy was noted in multiple cell lines including human osteosarcoma U2OS cells (Fig S3A of Supporting information), suggesting the effects of Rab25 on autophagy are generalizable. Autophagy requires the coordinate activity of multiple 'autophagy-related' proteins (Atg) including Atg6/Beclin1 that has been implicated in human breast, ovarian and prostate tumours cancer (Karantza-Wadsworth et al, 2007). Atg6/Beclin1 heterozygous mutant mice are tumour-prone implicating autophagy in tumourigenicity (Jin & White, 2007). However, expression of Atg6/Beclin1 was not significantly changed in response to Rab25 expression (Fig S3B of Supporting information).

5′-AMP-activated protein kinase (AMPK) is a major physiological sensor of intracellular energy levels. An increase in intracellular AMP/ATP ratio activates AMPK to maintain cellular energy balance (Kahn et al, 2005). As expected, following nutrient withdrawal, AMPK phosphorylation (pAMPK) increased as measured by both reverse phase protein arrays (RPPA; Fig 1E) and WB analysis (Fig 1F). However, the increase in pAMPK levels was markedly lower in Rab25-transfected cells following glucose and growth factor withdrawal (Fig 1E). AMPK, when activated, also phosphorylates acetyl CoA carboxylase (ACC) resulting in inhibition of energy-consuming fatty acid synthesis. AMPK phosphorylation levels paralleled ACC phosphorylation (pACC), as measured by RPPA (Fig 1G) and WB (Fig 1F). In keeping with the effect of Rab25 on AMPK phosphorylation, ACC phosphorylation was markedly decreased in cells expressing Rab25 (Fig 1F). Furthermore, Rab25 knockdown using RNAi sensitized cells to nutrient stress as indicated by increases in both basal- and nutrient deprivation-induced AMPK and ACC phosphorylation (Fig 1H).

Rab25 expression alters ATP levels

How does Rab25 expression reduce bioenergetic stress and delay the onset of autophagy under nutrient deprived conditions? Unexpectedly, Rab25 expression in cells grown in complete medium (RPMI1640 + 5% FBS) results in a consistent and statistically significant elevation of basal ATP levels compared to pcDNA-transfected cells (Fig 2A). The effects of Rab25 on ATP levels are even more striking during nutrient stress. Expression of Rab25 in A2780 or HEY ovarian cancer cells

Figure 2. Expression of Rab25 regulates cellular ATP and glycogen levels.

A. Expression of Rab25 increases endogenous ATP level in ovarian cancer cells. $^{*}p < 0.001$ Rab25 *versus* pcDNA. The mean cellular concentration of ATP per mg of protein (based on the standard curve generated using a known amount of ATP) is 2.36^{-10} moles/mg for IOSE29ht pcDNA cells, 6.21^{-10} moles/mg for IOSE29ht Rab25 cells, 8.14^{-11} moles/mg for IOSE80ht pcDNA cells, 1.05^{-10} moles/mg for IOSE80ht Rab25 cells, 2.85^{-10} moles/mg for A2780 pcDNA cells, 3.81^{-10} moles/mg for A2780 Rab25 cells, 7.23^{-10} moles/mg for HEY pcDNA cells and 9.82^{-10} moles/mg for HEY Rab25 cells.

B. Rab25 expression increases ATP synthesis and delays fall in total cellular ATP levels after glucose and serum withdrawal, $p < 0.001$ Rab25 *versus* control pcDNA.

C. Down-regulation of Rab25 expression decreases ability to maintain ATP after glucose and serum withdrawal (a) $p < 0.05$ SF-Glu *versus* FBS and (b) $p < 0.05$ *versus* control.

D. Expression of Rab25 increases total cellular glycogen content while down-regulation of Rab25 expression decreases total cellular glycogen content (μg of glycogen/mg protein). Cells were cultured in complete media for 24 h before glycogen measurement. (a) $p < 0.01$ Rab25 *versus* pcDNA, (b) $p < 0.05$ Rab25 RNAi *versus* NT RNAi and (c) $p < 0.05$ shRAb25 *versus* shRNA control.

E. Decrease in cellular glycogen content after glucose and serum withdrawal $^{*}p < 0.001$ Rab25 *versus* pcDNA.

F. Effect of GPi (Bay U6571) and oligomycin on ATP production. A2780 pcDNA transfected and Rab25 expressing cells were pretreated with vehicle (control), 30 μM of Bay U6571 (GPi) or 25 μg/ml of oligomycin for 2 h. Cells were then cultured in serum- and glucose free RPMI 1640 in the presence of absence of Bay U6571 or oligomycin for the indicated times. (a) $p < 0.01$ oligomycin time 0 *versus* control time 0 and (b) $p < 0.01$ *versus* time 0 at each treatment group.

G. Effect of Bay U6571 on cellular glycogen (left panel) and ATP (right panel) levels in HEY cells. (a) $p < 0.01$ *versus* pcDNA control time 0 at 5% FBS and (b) $p < 0.01$ GPi *versus* control at each corresponding treatment.

H. Down regulation of Rab25 expression and inhibition of glycogen breakdown by GPi administration increases 2DG induced cell death $^{*}p < 0.05$ *versus* shRNA control.

results in maintenance of higher ATP levels in the absence of glucose and FBS (growth factor deprivation) over at least 6 h and to a lesser degree over 24 h of culture (Fig 2B). Hence, the elevated ATP level in Rab25-expressing cells likely lowers the AMP/ATP ratio leading to decreased AMPK activation. Compatible with a role for Rab25 in maintaining ATP levels under nutrient stress, down-regulation of Rab25 in cells expressing endogenous Rab25 by shRNA (Fig 2C) or by RNAi (Fig S4A of Supporting information) significantly decreased ATP levels ($p < 0.01$).

The ability of Rab25 to maintain ATP levels following nutrient withdrawal without activation of autophagy could be due to the utilization of internal nutrient reserves such as glycogen, triglycerides or proteins, which can be rapidly metabolized for energy production (Greenberg et al, 2006). Cellular glycogen but not triglyceride or protein levels (data not shown) were significantly higher in Rab25-expressing cells grown in complete medium (Fig 2D). This is striking as glycogen has not been proposed to represent a major component of energy stores in epithelial cancer cells. Down-regulation of Rab25 expression

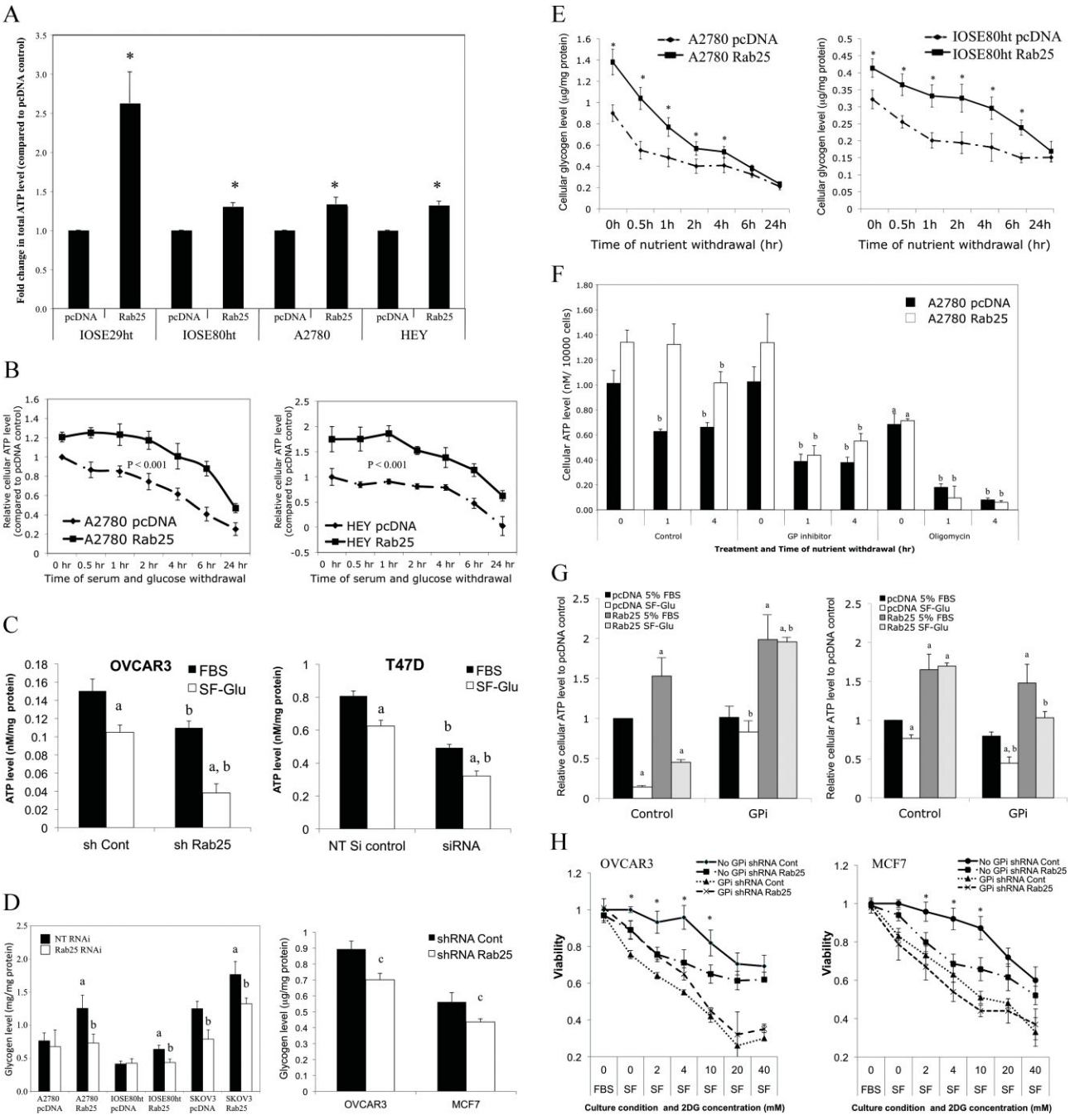

Figure 2.

using siRNA (left panel) or shRNA (right panel) reduced basal glycogen levels suggesting a role for Rab25 in controlling cellular glycogen production or storage. Following nutrient deprivation, glycogen levels fell rapidly, compatible with conversion to glucose for ATP synthesis (Fig 2E), suggesting that glycogen may contribute to the maintenance of cellular energy levels during metabolic stress in Rab25 expressing cells (Fig 2B).

Glycogen is converted to glucose-1-phosphate by glycogen phosphorylase (GP) and then to glucose-6-phosphate before entering the glycolytic pathway to produce ATP (Roach, 2002). We thus determined the effect of preventing conversion of glycogen to glucose-1-phosphate, by GP inhibition, on ATP levels. A2780 ovarian cancer cells expressing Rab25 or pcDNA-transfected cells were pretreated with 30 μM Bay U6571 GP inhibitor (GPi) or 200 ng/ml oligomycin (an ATP synthase inhibitor) for 4 h in complete media before nutrient withdrawal. Incubation of cells with the GPi in complete media did not significantly alter basal ATP levels (Fig 2F), presumably due to the high concentration of glucose in the media that can be utilized as an energy source. Strikingly, the presence of GPi essentially abrogated the ability of Rab25 to maintain cellular ATP levels after glucose deprivation (Fig 2F), indicating that the conversion of endogenous glycogen to glucose-1-phosphate plays a critical role in the ability of Rab25 to maintain elevated ATP levels during glucose deprivation. Blocking mitochondrial ATP production by oligomycin significantly decreased cellular ATP levels under all conditions suggesting that a significant component of the ATP production in Rab25-expressing cells is through oxidative phosphorylation (Fig 2F). The ability of the GPi to block glycogenolysis and decrease ATP levels during glucose deprivation was confirmed in Rab25-expressing HEY (Fig 2G) and MCF7 cancer cells (Fig S4B of Supporting information). Thus the elevated glycogen stores induced by Rab25 appear to maintain ATP levels during the early phase of metabolic stress. In agreement with the changes in cellular ATP levels, blocking glycogen catabolism by pretreating cells with the GPi elevated ACC phosphorylation above control levels in the absence of the GPi (Fig S4C of Supporting information). Functionally, addition of the glycolysis inhibitor 2DG induced cell death in both OVCAR3 and MCF7 cells (Fig 2H). Importantly, reducing Rab25 expression by shRNA-mediated knockdown increased cell death induced by low dosage 2DG (2–10 μM). Thus, blocking glycogenolysis and subsequent glycolysis reduce the ability of Rab25-expressing cells to maintain survival during early nutrient stress, implicating utilization of glycogen as an important energy source (Fig 2H).

Rab25 regulates cancer cell bioenergetics through an AKT-dependent pathway

Glycogen synthase (GS), which converts glucose into glycogen for storage, is inhibited by phosphorylation at several sites by GS kinase-3 (GSK3; Woodgett, 1994). GSK3, in turn, is inhibited by phosphorylation by AKT following PI3K pathway activation. We have previously reported that Rab25 expression is associated with a concomitant increase in AKT activation through a yet unexplored mechanism (Cheng et al, 2004). Consistent with our previous observations, AKT S473 phosphorylation, reflecting AKT activation, was markedly increased in Rab25-expressing cells leading to increased GSK3 phosphorylation and consequent decreases in GS phosphorylation in the presence or absence of serum (Fig 3A). To determine whether the activation of AKT and subsequent inhibition of GSK3 and consequent activation of GS play a role in determining intracellular glycogen levels, we examined the effect of inhibition of PI3K or GSK3 by PI103, a potent and selective inhibitor of class I PI3K (Raynaud et al, 2007) or GSK3i (SB-216763), respectively, on cellular glycogen levels. Cells were placed in complete media containing PI103 or GSK3i for 2 h to allow PI103 or GSK3i to enter cells, followed by a 2 h incubation in glucose- and foetal bovine serum (FBS)-free medium to induce a reduction in endogenous glycogen levels. WB demonstrated the efficacy of PI103 and GSK3i in inhibiting phosphorylation of AKT and GSK3, as well as decreasing phospho-GS levels (Fig 3B). The GPi Bay U6571 was included as a control for the specificity of effects of PI103 and GSK3i.

Treating A2780 pcDNA-transfected ovarian cancer cells with GSK3i, thus releasing inhibition of GS activity as a consequence of

Figure 3. Rab25 regulates bioenergetics in ovarian cancer cell through the AKT pathway.

A. Rab25 expression increases phospho but not total AKT and GSK3 levels in A2780 cells leading to decreased phosphorylation of GS (pGS).

B. WB analysis of AKT and GSK3 phosphorylation confirming the inhibitory effect of PI3K pathways inhibitors PI103, GPi and synthase kinase 3 inhibitor (GSK3i) in HEY cells.

C. Inhibition of GSK3 activity increases total cellular glycogen levels. pcDNA transfected and Rab25 expressing ovarian cancer cells were cultured in complete media in the presence of 10 μM GSK3i for the indicated times. Total cellular glycogen content was measured and normalized with total protein content. (a) $p < 0.001$ *versus* no GSK3i treated pcDNA cells.

D-E. Effect of PI3K inhibitor PI103 on cellular glycogen content and ATP production. Ovarian cancer cells were pretreated with PI103 for at least 2 h in complete media. Cells were then subjected to 2 h glucose and FBS withdrawal to deplete endogenous glycogen followed by culturing cells in RPMI-glucose media in the presence of PI103 for 2 h (2 h SF). After 2 h of nutrient stress, complete media containing PI103 was added to the cells for 30 min (5% FBS) for recovery. A second glucose and FBS withdrawal (15 min SF) followed immediately to examine the effect on glycogen and ATP levels. a, $p < 0.001$ 5% FBS *versus* 2 h SF, b, $p < 0.01$ 15 min SF *versus* 5% FBS.

D. There is an increase in glycogen content during recovery phase (5% FBS) and a decrease in glycogen when cells are subject to a second nutrient stress (15 min SF).

E. Utilization of glycogen to produce ATP.

F. Addition of AKT inhibitor MK2206 (AKTi) abolishes Rab25-dependent glycogen storage. (a) $p < 0.05$ *versus* shRNA control and (b) $p < 0.01$ SF + AKTi *versus* SF.

G. Inhibiting AKT pathway and glucose metabolism decreases cell viability. Cells were pretreated with 10 μM of PI103 or AKTi, 100 μM LND or 3BrPy for 2 h before switching to SF media in the presence of inhibitors for an addition16 h before cell titre blue viability assay. $^{*}p < 0.001$ shRNA Rab25 *versus* shRNA control.

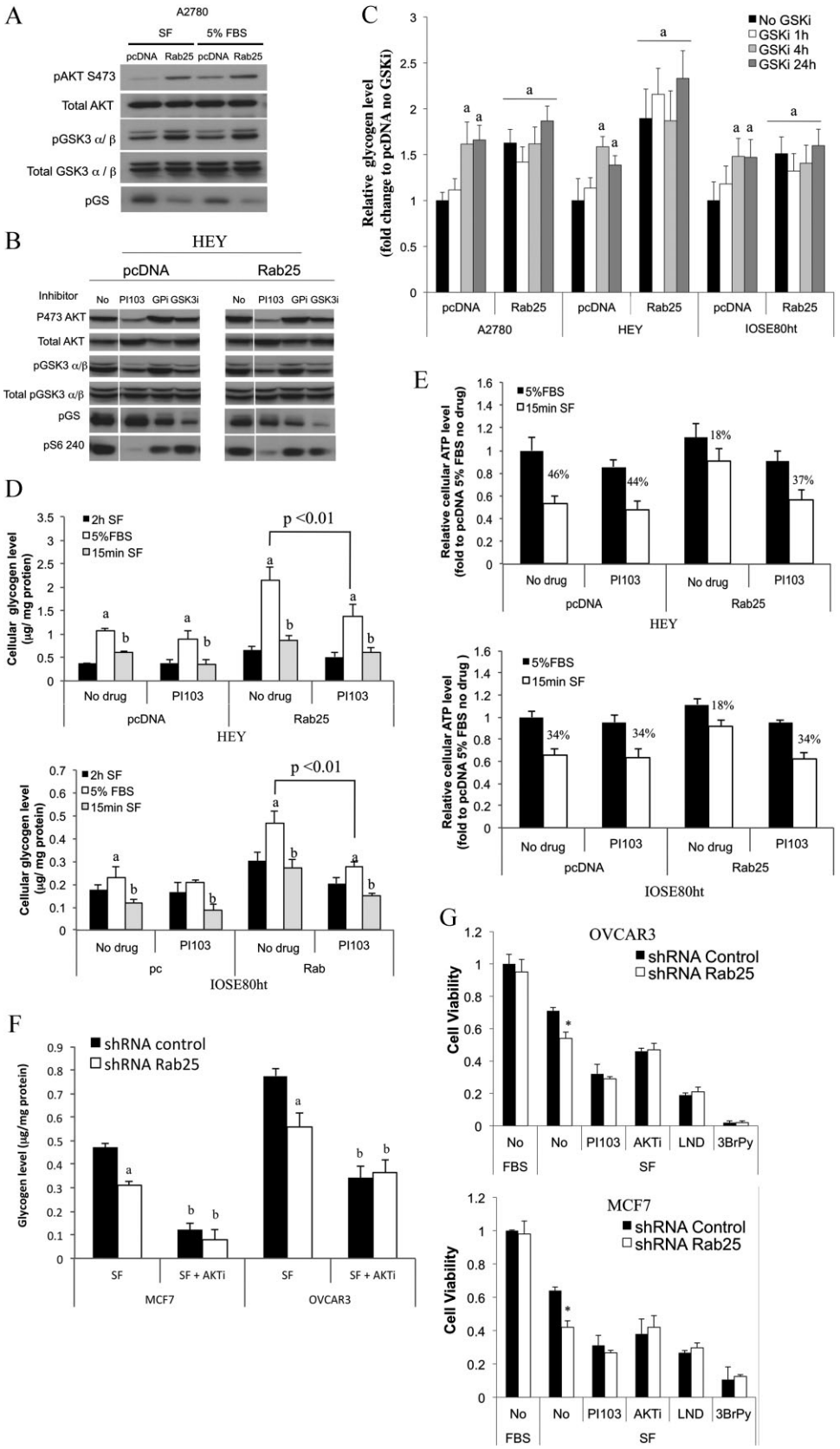

Figure 3.

GSK3-mediated phosphorylation, increased cellular glycogen content to levels observed in Rab25-expressing cells (Fig 3C). In contrast, GSK3i had minimal effects in Rab25-expressing cells compatible with GSK3 inhibition as a consequence of Rab25-induced AKT activation (Fig 3C). Similar results were observed in HEY and IOSE80ht cells where GSK3i increased glycogen levels ($p < 0.05$) in pcDNA-transfected cells, whereas, a significant change in glycogen levels was not observed in Rab25-expressing cells (Fig 3C). Thus, increased AKT activity with subsequent inhibition of GSK3 in Rab25-expressing cells likely contributes to increased GS activity and glycogen accumulation.

PI103 did not alter the modest glycogen accumulation that occurred in pcDNA-transfected HEY or IOSE80ht cells returned to nutrient- and FBS-replete media (Fig 3D). In both HEY and IOSE80ht cells, Rab25 expression markedly increased the accumulation of glycogen in cells released from starvation ($p < 0.01$). When cells were subjected to a second nutrient stress, glycogen levels fell rapidly (Fig 3D) suggesting that the glycogen stored during the short incubation in glucose- and serum-replete media provides an immediate source of energy. The role of the PI3K–AKT pathway in maintaining cellular ATP levels in Rab25 expressing cells was assessed using PI103. The ability of Rab25 to induce glycogen accumulation (Fig 3D) and maintain ATP levels (Fig 3E) under stress was compromised in the presence of PI103, compatible with Rab25 increasing glycogen stores and maintaining ATP levels during nutrient stress through Rab25-mediated PI3K pathway activation (Fig 3D and E).

These observations were further evaluated in OVCAR3 and MCF7 cells using shRNA-mediated stable knockdown of Rab25 expression, which decreased basal glycogen levels (Fig 3F and Fig S5A of Supporting information). The specific AKT inhibitor (MK2206) significantly decreased glycogen levels further and indeed overrode the effects of Rab25 shRNA supporting a role for AKT activation in Rab25-induced glycogen accumulation (Fig S5A of Supporting information). When cells were cultured in serum-free conditions, wherein, AKT activation by exogenous stimulation is absent, cells expressing Rab25 maintained elevated basal glycogen levels, whereas, Rab25 shRNA induced a decrease in glycogen levels (Fig 3F). MK2206 markedly decreased glycogen levels and abrogated the effect of Rab25 shRNA (Fig 3F). Similar results were obtained in T47D cells treated with Rab25 siRNA or with MK2206 (Fig S5B of Supporting information).

Culturing OVCAR3 and MCF7 cells in serum-free medium led to a decrease in cell survival (Fig 3G). Knocking down Rab25 levels augmented the cell death (Fig 3G). Inhibition of PI3K or AKT activity with PI103 or MK2206, respectively, resulted in similar levels of cell death regardless of the presence of Rab25 shRNA supporting a Rab25/PI3K/AKT-dependent mechanism for Rab25-mediated cell survival (Fig 3G). Addition of lonidamine (LND) or 3-bromopyruvate (3BrPy), two potent glycolysis inhibitors (Pelicano et al, 2006), also significantly decreased cell viability supporting the dependence on glucose as an energy source for cell survival.

Cellular glycogen synthesis depends on intracellular glucose. Glucose uptake, assessed using tritium-labelled 2DG in cells maintained in Krebs–Ringers phosphate solution (*i.e.* growth factor and glucose depleted environment), was significantly higher in Rab25-expressing cells than in parent cells (Fig 4A). Similarly down-regulation of Rab25 decreased glucose uptake (Fig 4B). AKT activation has been demonstrated to increase glucose uptake (Tong et al, 2009). Indeed, treating Rab25 over-expressing HEY cells with MK2206 effectively inhibited cellular glucose uptake regardless of the presence or absence of Rab25 (Fig 4B). Similarly, AKT-specific siRNA (Fig S5C of Supporting information) decreased glucose uptake, supporting a critical role for AKT in Rab25-induced glucose uptake. MK2206 further reduced glucose uptake (Fig 4B) in the presence or absence of Rab25 or AKT siRNA further supporting a role for AKT Rab25 function. Likewise, knockdown of endogenous Rab25 or inhibiting AKT activity in OVCAR3 and T47D cells using specific shRNA or MK2206, respectively, significantly reduced glucose uptake ($p < 0.001$) confirming a role for AKT in regulation of glucose uptake by Rab25 (Fig 4C).

In rat cardiomyocytes, Rab11, the closest Rab family member to Rab25 (by sequence homology), colocalizes with glucose transporter (GLUT) 4-containing vesicles and redistributes to the plasma membrane with GLUT4 (Watson et al, 2004). We, therefore, reasoned that Rab25 could contribute to GLUT trafficking. As GLUT1 is the primary GLUT expressed in ovarian cancer cells (Rudlowski et al, 2004), we examined the localization of GLUT1 and Rab25 by immunofluorescence staining under nutrient stress and nutrient-replete conditions in

Figure 4. Rab25 increases glucose uptake.

A. Rab25 over-expression increases H^3-labelled 2DG uptake. (a) $p < 0.001$ Rab25 *versus* pcDNA. Results are mean ± s.d. of a triplicate in one of representative experiment.

B. Down-regulation of Rab25 or AKT expression, or inhibition AKT activity by MK2206 decreases glucose uptake in HEY cells (a) $p < 0.001$ *versus* NT siRNA control, (b) $p < 0.05$ *versus* siRab25 and (c) $p < 0.05$ *versus* siAKT.

C. Effect of down regulation of Rab25 and AKT inhibitor MK2206 (AKTi) on glucose uptake. Cells were either pretreated for 2 h with AKTi before assessing glucose uptake. (a) $p < 0.05$ *versus* shRNA control and (b) $p < 0.05$ *versus* shRab25.

D. Rab25 co-localization with GLUT1 in A2780 cells. Immunofluorescent staining of GLUT1 (red) and Rab25 (green). Co-localization of GLUT1 and Rab25 (*i.e.* yellow) is indicated by arrows. Single scale bar, 10 μM.

E-G. Resistance to 2DG induced cell death in Rab25 cells is mediated through the PI3K/AKT pathway. Inhibition of the PI3K/AKT pathway was achieved by addition of 10 μM of PI103 or MK2206.

E. AKT inhibition increases sensitivity to 2DG induced cell death. $^*p < 0.001$ *versus* HEY pcDNA cells.

F. Down-regulation of AKT by siRNA specific to AKT.

G. Or down-regulation of Rab25 by shRNA specific to Rab25 enhances 2DG induced cell death. $^*p < 0.001$ *versus* RNAi control cells.

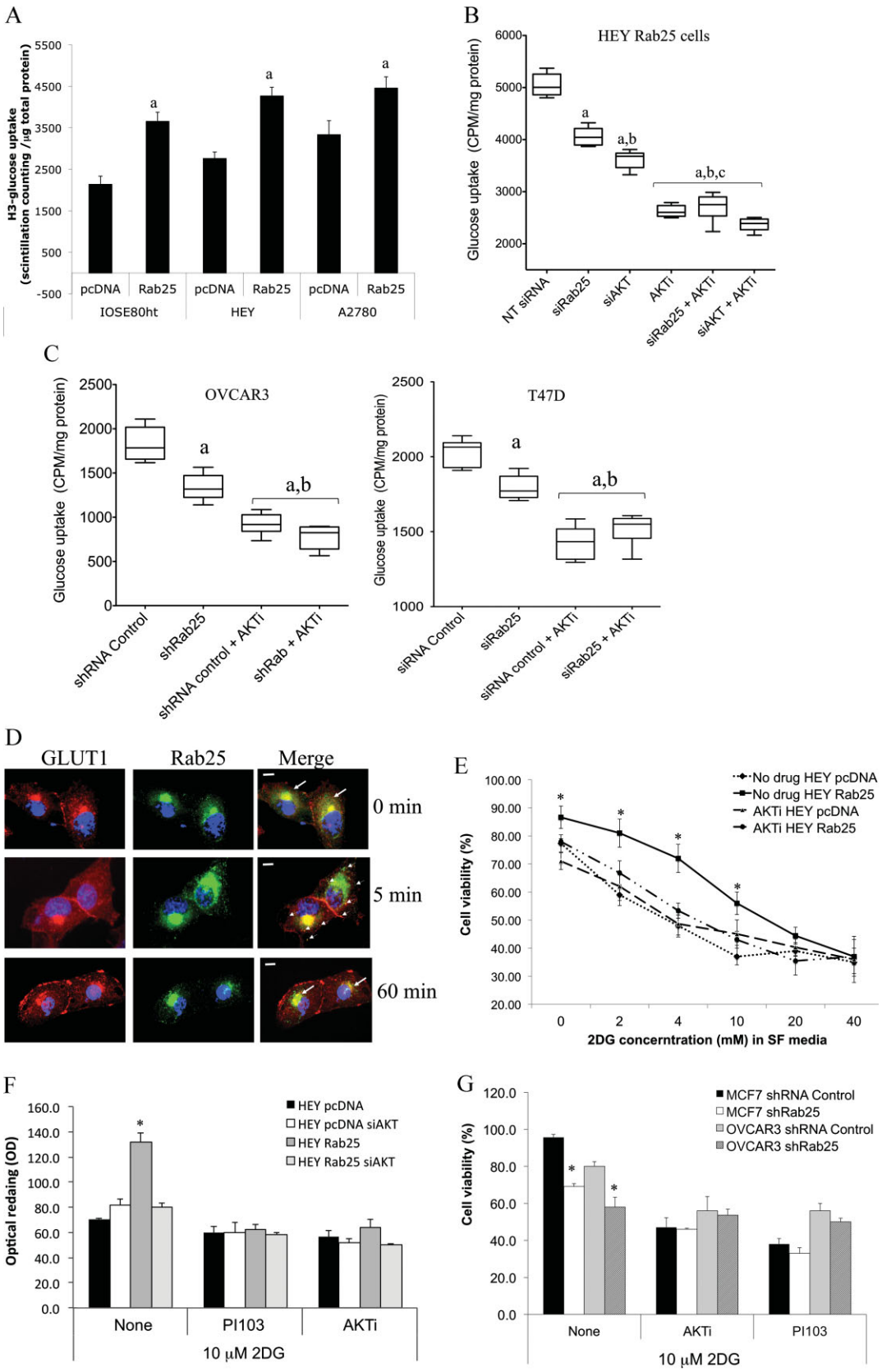

Figure 4.

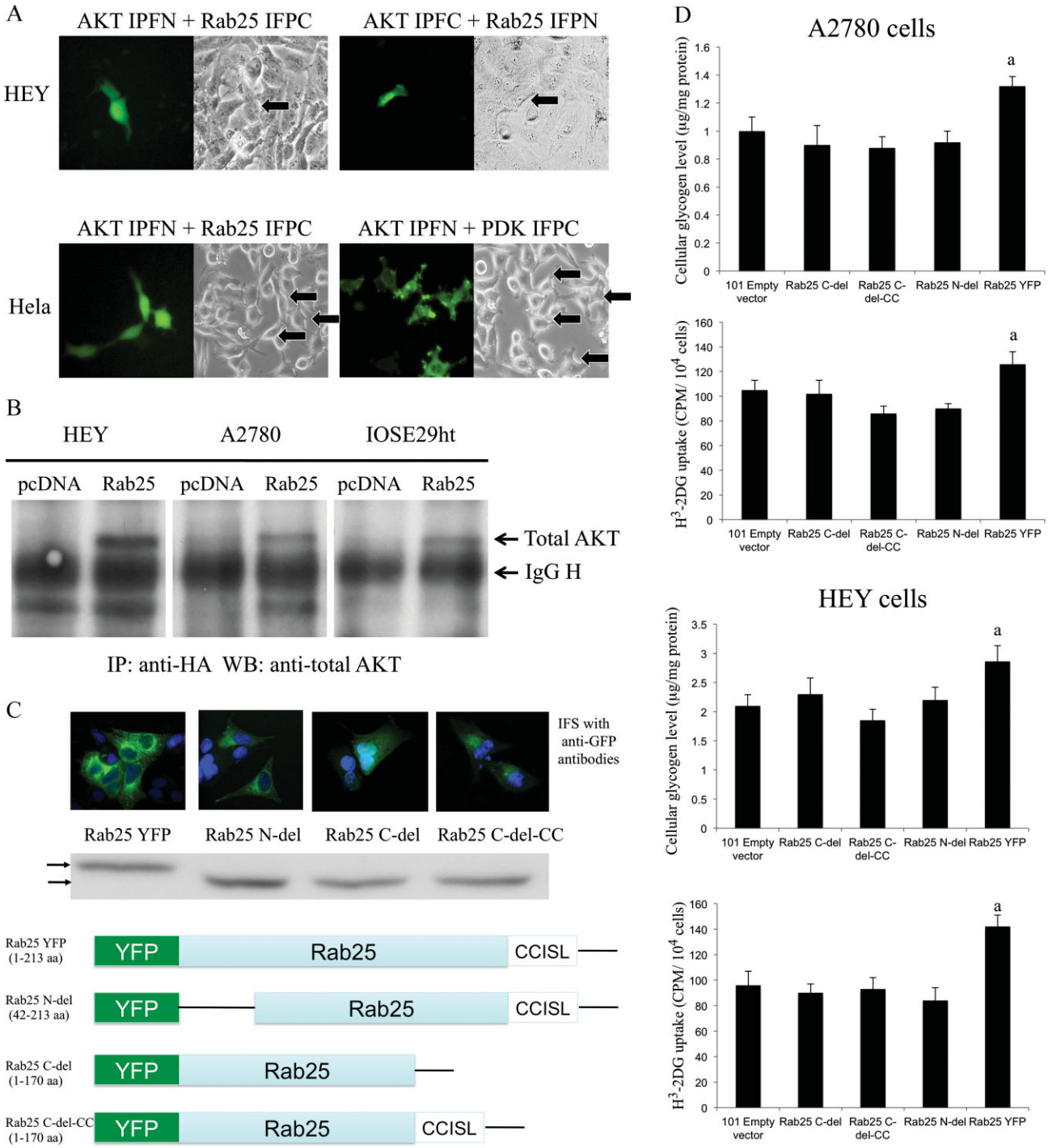

Figure 5. Detection of physical association between AKT and Rab25 by protein complementation assay (PCA).

A. Ovarian cancer HEY cells (upper panel) were co-transfected with AKT-IFPN and Rab25-IFPC or with AKT-IFPC and Rab25-IFPN. Cells become fluorescent due to an interaction between AKT and Rab25 bringing the two halves of the fluorescent protein into proximity creating a stable complex and restoring fluorescence. Hela cells stably expressing AKT-IFPN (lower panel) were transfected with Rab25-IFPC or PDK-IFPC as control. A brightfield image corresponding to the fluorescent image is shown and transfected cells indicated by an arrow.

B. Detection of Rab25 and AKT interaction by immunoprecipitation. Ovarian cells expressing HA-tagged Rab25 were IP with anti-HA antibody. The resultant complex was separated by gel electrophoresis and detected by WB using anti-AKT antibody.

C. Generation of Rab25 deletion mutants. Expression of the deletion mutants was detected by immunofluorescence staining (upper panel) and WB (middle panel) using anti-GFP antibody which interacts with YFP. Diagrammatic representation of the structure of the mutants is shown in the lower panel.

D. Rab25 deletion mutants do not alter cellular glycogen and ATP levels. Ovarian cancer cell lysates were collected 24 h post transfection. (a) $p < 0.05$ versus empty vector transfected cells.

A2780 cells (Fig 4D). When cells were cultured in the absence of glucose and growth factors, GLUT1 co-localized with Rab25 in a perinuclear distribution (Fig 4D). Addition of FBS as a source of growth factors and glucose for 5 min resulted in redistribution of a portion of GLUT1 from a perinuclear location to the cytoplasmic membrane. Importantly, Rab25 colocalized with GLUT1 during the translocation process (as indicated by arrows) suggesting that GLUT1 may represent a Rab25 cargo.

High AKT activity has been reported to render cells more susceptible to death induced by glucose withdrawal or treating with a glycolysis inhibitor (Elstrom et al, 2004; Fan et al, 2010; Kurtoglu et al, 2007). Thus, Rab25 expression, with subsequent increases in AKT activation and glucose uptake, would be expected to increase sensitivity to 2DG-induced cell death. However, as noted above, Rab25 expression decreased sensitivity of HEY cells to low doses of 2DG (2–10 μM), whereas, high doses of 2DG (20–40 μM) led to similar levels of cell death in parental and Rab25-transfected HEY cells (Figs 2H and 4E). Decreasing expression of Rab25 or activity of AKT by siRNA specific to Rab25 (Figs 2H and 4F) or MK2206 (Fig 4E), respectively, increased cellular sensitivity to 2DG-induced cell death. Interestingly, 2DG has been reported to activate the AKT signalling pathway and protect cancer cells from death (Zhong et al, 2008, 2009). To further evaluate the relationship between Rab25 and AKT in the response to 2DG, we examined AKT activation in OVCAR3 and MCF7 cells. 2DG induced an increase in AKT phosphorylation in both cell lines in a dose- and time-dependent manner similar to the results reported by Zhong and colleagues. Down-regulation of Rab25 levels reduced AKT activation, compatible with Rab25 regulating AKT activation (Fig S5D and E of Supporting information). As expected, culturing OVCAR3 or MCF7 cells in 2DG decreased cell viability, a process that was augmented by siRNA to Rab25 (Fig 4G). Importantly, the addition of AKT or PI3K inhibitors further decreased cellular viability independently of the presence or absence of Rab25 siRNA compatible with the PI3K/AKT pathway mediating the effects of Rab25 on cellular viability (Fig 4G).

Interaction of Rab25 with AKT is required for effects of Rab25 on cellular metabolism

A protein complementation-based assay (see Materials and Methods Section of Supporting information for details), wherein, reconstitution of fluorescence is dependent of protein–protein binding bringing two fragments of a GFP-like molecule into proximity, demonstrated the association of Rab25 with AKT (Fig 5A). Transient transfection of: (1) AKT-IFPN (intensely fluorescent protein amino-terminal half) and *RAB25*-IFPC (intensely fluorescent protein carboxy-terminal half) or (2) AKT-IFPC and *RAB25*-IFPN fusion proteins in HEY ovarian cancer cells resulted in fluorescence indicating association of AKT and Rab25 protein in the PCA complex (Fig 5A upper panel, double transfected cell indicated by arrow). No fluorescent cells were observed in other control conditions including (AKT-IFPC and IFPN), (AKT-IFPN and IFPC) as well as (Rab25 IFPC and ACTN4-IFPN) indicating a specific binding of Rab25 with AKT (Fig S6 of Supporting information). We further confirmed the association of Rab25 with AKT using PCA in AKT-IFPN stably expressing HeLa cells by transient transfection of a Rab25-IFPC construct (Fig 5A, lower panel). 3-phosphoinositide-dependent protein kinase-1 (PDK1), a well-established AKT binding partner, was included as a positive control. In support of an interaction between AKT and Rab25, AKT and Rab25 could be co-immunoprecipitated (IP) in ovarian cancer cells expressing Rab25 (Fig 5B).

To elucidate the molecular mechanism by which Rab25 interacts with AKT, Rab25 deletion mutants were designed (Fig 5C). Expression of these deletion mutants was demonstrated by WB and immunofluorescence staining using anti-GFP antibody (Fig 5C). Wild-type Rab25-YFP localizes to the perinuclear region similar to endogenous Rab25 (Fig 5C). Deletion of 43 amino acids from the C-terminal (Rab25-C-del) of Rab25, containing the putative geranylgeranyl transferase II acceptor motif CCISL, results in a diffuse distribution of Rab25 throughout the cytosol, while addition of a CCISL motif to Rab25-C-del (Rab25 C-del-CC) restores the normal Rab25 perinuclear distribution implicating the CCISL motif in Rab25 localization. Deletion of 41 amino acids from the N-terminus of Rab25 (Rab25 N-del) did not affect localization (Fig 5C). However, no observable fluorescent complex formed when any of the mutants were coexpressed with AKT as assayed by the PCA methodology (data not shown). Thus, a full length Rab25 able to localize to the correct compartment appears necessary to interact with AKT. Strikingly, transient expression of each of the mutants that are unable to bind AKT, in contrast to full length Rab25 YFP that binds AKT, into ovarian cancer cells did not alter cellular glycogen levels or glucose uptake (Fig 5D), supporting the contention that interaction of Rab25 with AKT is likely required for the ability of Rab25 to alter glucose uptake and glycogen storage.

Elevated Rab25 levels in patient samples are associated with altered cellular bioenergetics

To determine whether the effects of Rab25 on cellular stress observed in cell lines also occurred in human tumours, we measured Rab25, total AKT, total AMPK, total ACC, total GS, pAKT (T308), pAMPK, pACC and pGS protein levels in tumour lysates from 667 ovarian cancer specimens using RPPA. As expected, due to ACC being an AMPK target, a positive correlation (Spearman, $p = 1.007161e{-}32$) was observed between pAMPK and pACC protein levels in ovarian cancer tissues. This positive correlation also served to validate the ability to accurately assess pAMPK and pACC in patient samples. Recapitulating the *in vitro* data, there was a highly significant inverse correlation between Rab25 levels and pAMPK ($p = 0.00015$), pACC ($p = 7.93e{-}12$) and pGS ($p = 0.00001$) as well as a positive correlation ($p = 1.34e{-}9$) between Rab25 and pAKT in patient samples. We did not examine the potential correlation between pGSK3 and Rab25 as available phosphoGSK3 antibodies detect both alpha and beta forms of GSK3 as well as p90RSK mitigating its utility in RPPA. Furthermore, we observed a positive correlation ($p = 0.032$) between cellular glycogen content and expression of Rab25 in 31 ovarian patient tumour samples (Fig 6A). Thus, the effects of Rab25 on cellular metabolism *in vitro* are recapitulated in ovarian cancer in the patient.

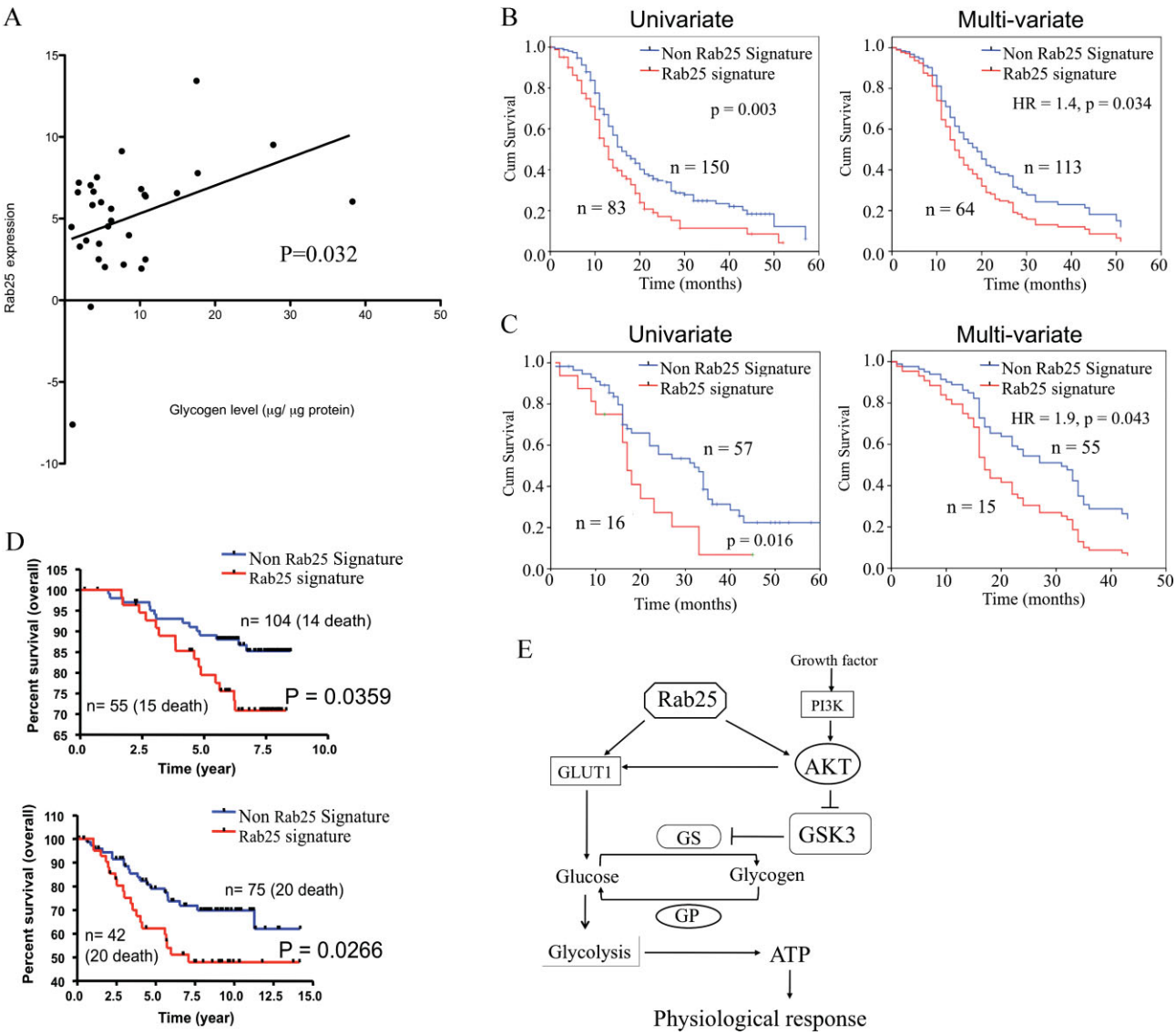

Figure 6. Prediction in clinical samples.

A. Rab25 expression correlates with glycogen levels in patient tumours. Total RNA and total cellular extracts, isolated from 31 ovarian cancer patient specimens, were subjected to Rab25 gene expression and glycogen content analysis using QPCR and glycogen assay, respectively.

B–C. The Rab25 expression signature identifies patients with a poor prognosis. Ovarian cancer patients were classified as either mirroring the Rab25-associated gene expression signature (Rab25 signature) or not (non-Rab25 signature) using linear discriminant analysis in BRB tools, in two independent published ovarian datasets. Progression free survival curves for patients with advanced disease (Stage II to IV) are shown. Univariate analyses were plotted using Kaplan-Meier method and Coxplots used for multivariate analyses (co-variates included stage, grade, histology and residual disease).

B. Tothill et al, 2008.

C. Dressman et al, 2007.

D. Prediction of breast cancer overall survival in two independent published breast datasets (upper panel) Pawitan et al, 2005 and (lower panel) Chin et al, 2006, based on Rab25-associated gene signature. Breast patient classification was determined by BRB tool class prediction function to identify patient with Rab25-associated gene expression signature (Rab25-signature) or without (non-Rab25 signature). All patients from the datasets were included in class prediction.

E. Proposed model for the mechanism by which Rab25 regulates cellular bioenergetics.

To assess the potential clinical relevance of the Rab25-dependent transcriptional profile and the effect of Rab25 on cellular metabolism, we classified serous ovarian cancers into Rab25-like and pcDNA-like based on their expression patterns in two large-independent publically available datasets (Dressman et al, 2007 and Tothill et al, 2008, see External Datasets Section of Supporting information for details) using approaches described previously (Lee et al, 2006). Using linear discriminant analysis, leave-one-out cross validation, and cell lines with and without Rab25 expression as the training set, a Rab25-dependent

gene signature – consisting of 62 probes for 53 genes (Table S3 of Supporting information) from the original 1167 probesets (Fig S1 of Supporting information) – was used to classify ovarian cancers as Rab25-like in the Tothill et al (Fig 6B) and Dressman et al (Fig 6C) datasets. Rab25-like cancers were associated with significantly higher rates of relapse (Fig 6B) and poorer survival (Fig 6C). Furthermore, the Rab25 signature was an independent prognostic factor in multivariate analysis (Fig 6B and C), in keeping with a role for Rab25 in modulating aggressiveness of ovarian cancer. We previously demonstrated that Rab25 levels alone predict survival only in the subset of patients with very high and very low levels of Rab25 (Cheng et al, 2004). In contrast, the Rab25 signature was able to predict outcomes for all ovarian cancer patients indicating that the Rab25-dependent signature contains important information related to ovarian cancer pathophysiology not captured by Rab25 levels alone. Intriguingly, this signature is not only highly portable from cell lines to clinical ovarian tumour samples, but also proved to be a strong predictor of survival in breast cancer samples (Fig 6D) using two-independent datasets (Pawitan et al, 2005 and Chin et al, 2006, see External Datasets Section of Supporting information for details), further supporting the role of Rab25 in aggressiveness of cancers.

Collectively, our data implicate Rab25 in glucose and glycogen metabolism. The effects of Rab25 appear to be mediated, at least in part, through an interaction between Rab25 and AKT leading to increased glucose uptake, which combined with AKT-induced inhibition of GSK3 and increase in GS activities results in higher basal glycogen and elevated ATP levels. The increased glycogen stores, in turn, provide an alternative energy source during early nutrient stress reducing sensitivity to nutrient stress and increasing cell survival (Fig 6E).

DISCUSSION

RAB25 is amplified as part of the 1q22 amplicon in multiple cancer lineages. In support of an oncogenic function for Rab25, we have previously demonstrated worsened outcomes for ovarian and breast cancer patients whose tumours have markedly elevated Rab25 levels (Cheng et al, 2004). Further, increased Rab25 levels markedly increased tumour growth in xenograft models. Similarly, knockdown of Rab25 expression by RNAi decreases growth of ovarian cancer xenografts (Fan et al, 2006). Rab25 promotes $\alpha5\beta1$ integrin-containing vesicle trafficking to the membrane of pseudopodal tips, thereby, facilitating cell invasion (Caswell et al, 2007) potentially contributing to the aggressiveness of ovarian cancer. A recent study further demonstrated that overexpression of Rab25 in rat intestinal cells can lead to microtubule-dependent transformation *in vitro* and tumour formation *in vivo* (Lapierre et al, 2011). However, other studies have suggested that Rab25 may act as a tumour suppressor under some contexts. Loss of Rab25 in some triple-negative cell lines (Cheng et al, 2010) promotes tumourigenicity, and a recent study has reported an increase in colonic tumour incidence in Rab25-deficient mice bred into an APCmin/+ genetic background (Nam et al, 2010). Indeed, we have previously demonstrated that Rab25 is not sufficient to transform immortalized but non-tumourigenic cells (Cheng et al, 2004) and similarly, Rab25-knockout mice do not exhibit significant anatomical and pathological abnormalities (Nam et al, 2010). Consequently, Rab25 may not play a role in tumour initiation either as a primary oncogene or tumour suppressor gene, but rather may function as a regulator of tumour progression in already transformed cells. Thus, the effects of Rab25 appear to be context-dependent. Rab25 may exert different effects dependent on the intrinsic expression patterns in different cell lineages, the presence of different underlying genomic aberrations, the levels of specific Rab25 molecular partners, the cargoes being transported in Rab25-containing vesicles or the response of cells to activation of the signal transduction pathways controlled by Rab25. Context-dependent effects on tumour initiation and progression are not without precedence with both autophagy (Eisenberg-Lerner & Kimchi, 2009) and TGF beta (Chaudhury & Howe, 2009) demonstrating tumour inhibiting and promoting activity in different circumstances. In the present study, we manipulated Rab25 levels with a combination of enforced expression and knockdown to elucidate the mechanisms underlying Rab25 function. We identified a Rab25-associated gene signature using A2780 ovarian cancer cells *in vitro*. The Rab25 transcriptome was capable of identifying ovarian cancer patients with a poor prognosis with high confidence. Importantly, we observed a novel role of Rab25 in cellular survival and, in particular, in regulating cellular metabolism.

Increased glucose consumption is a characteristic of malignant cells. However, early studies noted *in vivo* that the amount of glucose uptake in tumours was too high to be utilized solely through glycolysis (Gullino et al, 1967). Our current data show that increased Rab25 expression decreases sensitivity to nutrient stress. Rab25-expressing cells demonstrated an unexpected and unprecedented increase in cellular glycogen stores. The elevated glycogen content in cells with high Rab25 levels is recapitulated *in vivo* in patient tumour samples. Glycogen stores have not previously been proposed as a viable energy source that could contribute to the ability of epithelial cancer cells to withstand nutrient stress. Indeed other than clear cell tumours where glycogen stores are prominent, the ability to store and utilize glycogen as an energy source has not been implicated in epithelial tumourigenesis and represents a novel observation in the context of cancer biology.

Our data suggest that Rab25 may increase glycogen stores and ATP levels, in part, by increasing glucose uptake. GLUT1 is over-expressed in multiple solid tumours and high GLUT1 levels have been associated with poor patient survival (Rudlowski et al, 2004). Strikingly, Rab25 colocalizes with GLUT1 suggesting a potential role for Rab25 in regulating translocation of GLUT1 to the membrane thus enhancing glucose uptake. Rab25-mediated activation of AKT may further enhance glucose uptake. The increased glucose uptake under nutrient-rich conditions in Rab25-expressing cells is associated with elevated glycogen stores, the mobilization of which is sufficient to explain, at least in part, the maintenance of ATP levels during acute bioenergetic stress.

GSK3 is a key and potent regulator of GS activity. Expression of Rab25 increased AKT activity (Cheng et al, 2004), which led to increased GSK3 phosphorylation, and subsequent inhibition of GSK3 activity as demonstrated by decreased GS phosphorylation. Together, this cascade provides an additional mechanism by which Rab25 could increase glycogen synthesis resulting in glycogen accumulation. Indeed, inhibition of PI3K decreased the ability to Rab25 to induce glycogen accumulation and inhibition of GSK3 recapitulated the ability of Rab25 to increase glycogen storage.

A full length functional Rab25 including the C-terminal geranylgeranylated motif is required to regulate cancer cell bioenergetics, at least as compared to either N- or C-terminal deletion mutants. Newly synthesized Rab proteins must be geranylgeranylated at C-terminal cysteine residues prior to anchoring to cellular membranes (Pereira-leal & Seabra, 2000). In agreement with this requirement, deletion of the C-terminus of Rab25 (Rab25-C-del) including the putative geranylgeranylated motif (CCISL) led to mislocalization of Rab25. Addition of the CCISL motif to the C-terminal truncation mutant was sufficient to restore normal Rab25 localization. Deletion of the N-terminus of Rab25 did not disturb subcellular localization compatible with the CCISL motif playing a key role in Rab25 localization. However, none of the Rab25 mutants retained the ability to interact with AKT, or to increase ATP, glycogen content and glucose uptake compatible with these processes being dependent on AKT activation. It is likely that the deletion mutants of Rab25 caused a change in availability of important functional motifs. For instance, the Rab25-N-del mutant lacks several functional domains, including RabSF1, RabSF2 and RabF1, the structural β-sheet and α-helix as well as 2-conserved G box (GDP/GTP-binding motif elements) that are implicated in GTP and downstream effector binding (Colicelli, 2004; Itzen & Goody, 2011; Pereira-leal & Seabra, 2000). Likewise, the deletion of the C-terminus of Rab25 deletes domains that interact with the Rab escort protein and Rab GDP-dissociation inhibitor (Itzen & Goody, 2011; Pereira-leal & Seabra, 2000). Additional fine mapping may further elucidate the functional domains of Rab25 required for the interaction of Rab25 with AKT and functional effects of Rab25. Overall, the coordinate effects of Rab25 mutation on AKT binding and ATP levels, glycogen content and glucose uptake suggests that the ability of Rab25 to bind and regulate AKT plays a critical role in the ability of Rab25 to regulate cellular bioenergetics, a contention supported by the PI3K, AKT and GSK3 inhibitor studies. In particular, it is worth noting that the addition of PI103 or MK2206 abolished the ability of Rab25 to increase cellular viability supporting the dependence of Rab25 activity on a functional PI3K/AKT pathway.

It has been reported that cells with high level of AKT activity are more sensitive to glucose withdrawal or glycolysis inhibition induced cell death induced (Elstrom et al, 2004; Fan et al, 2010; Kurtoglu et al, 2007). Inhibiting glycolysis by 2DG has been demonstrated to promote nutrient stress-induced cell death and to enhance the therapeutic efficacy of chemotherapeutic drugs (Simons et al, 2009). Interestingly, we have observed a decrease sensitivity of Rab25 expressing cells to low doses of 2DG (2–10 μM) despite elevated AKT activity in these cells. Hence, it is possible that under the submaximal dose of 2DG (10 μM), Rab25 may alter metabolism through pathways parallel to Akt to influence the outcome of cellular responses. Further, the discrepancy may also due to the nature of different cells or systems used in these studies. In addition, other studies have suggested that inhibition of glycolysis is not sufficient to explain the actions of 2DG on cell survival (Ralser et al, 2008). Further, 2DG has been shown to activate AKT and prevent cell death (Zhong et al, 2008; Zhong et al, 2009). Indeed, lung cancer cells with low levels of AKT activity were more susceptible to 2DG-induced cell death (Wangpaichitr et al, 2008). In the present study, we observed an increase in AKT activation in Rab25-expressing cells after 2DG administration, and inhibition of AKT by MK2206 increased cell death in response to 2DG, implicating AKT in preventing 2DG-induced cell death. AKT has been suggested to protect cells from 2DG-induced cell death by negatively regulating AMPK activity (Hahn-Windgassen et al, 2005; Memmott & Dennis, 2009; Priebe et al, 2011). Compatible with this observation, pAMPK and pACC are decreased in the presence of Rab25. Activation of mitochondrial-bound hexokinase (Gottlob et al, 2001), or by inhibiting *N*-linked glycosylation under normoxia, independent from glycolytic inhibition (Kurtoglu et al, 2007) have also been proposed as alternative mechanisms by which AKT protects cells from 2DG-induced death. Together, these studies suggest that a complex intracellular response governs the outcome of 2DG cytotoxicity.

It is noteworthy that expression of Rab25 delays induction of autophagy, which can function as an alternative form of non-apoptotic cell death under conditions of nutrient deprivation. The ability of Rab25 to increase basal ATP levels and to maintain ATP levels under early glucose- and serum-deprived conditions likely plays a major role in preventing the induction of autophagy. Defects in autophagy have been associated with increased tumourigenesis (Degenhardt et al, 2006; Liang et al, 1999). Metabolic stress can drive tumour cells with both defects in autophagy and apoptosis into necrotic cell death (Degenhardt et al, 2006). Diverting cells to necrotic cell death induces inflammatory cell infiltration and cytokine signalling (Proskuryakov et al, 2003), which by analogy with the wound healing process, may facilitate cell proliferation and angiogenesis favouring tumour growth (de Visser et al, 2006). In addition, defects in autophagy may allow accumulation of chromosomal instability and genomic mutation, as demonstrated by the higher rates of gene amplification and DNA damage observed in renal (Mathew et al, 2007) and mammary epithelial cells in response to metabolic stress when both apoptosis and autophagy were suppressed (Karantza-Wadsworth et al, 2007). However, following prolonged bioenergetic stress, ATP levels decrease in Rab25-expressing cells, AMPK becomes activated and cells eventually enter autophagy. Thus, Rab25 improves cellular bioenergetics sufficiently to delay the decrease in intracellular energy levels that induce entry into autophagy.

In conclusion, high levels of Rab25 appear to confer a functional advantage to cancer cells allowing cellular survival under acute nutrient stress conditions. In addition, a significant proportion of ovarian and breast cancers display a Rab25-

The paper explained

PROBLEM:

Despite progress in molecular medicine, cancer remains one of the leading causes of death. This is due to a failure to diagnose disease at an early curable stage as well as to the lack of effective therapeutic approaches. Alterations in the RAB small GTPases and the vesicle recycling processes they control contribute to multiple human diseases including cancer. RAB25, located in the 1q22 amplicon prevalent in many cancers, contributes to the aggressiveness of breast and ovarian and likely other cancer lineages. However, the molecular mechanisms underlying the effects of Rab25 on cancer pathophysiology remain unclear.

RESULTS:

To explore the mechanisms by which Rab25 alters cancer cell behaviour, we identified a RAB25 transcriptome. Importantly, the Rab25 signature is transferrable allowing interrogation of tumour samples and identification of patients with a poor prognosis. The Rab25 transcriptome is highly enriched in genes involved in cellular metabolism and survival. Indeed, Rab25 potently increases cancer cell survival under nutrient stress via increased AKT activation and subsequent glucose uptake, glycogen storage and maintenance of cellular bioenergetics. The data implicate an unexpected Rab25-induced increase in glycogen stores providing an energy source used during cell stress as a novel mechanism by which Rab25 could contribute to increased tumour aggressiveness and worsened patient outcomes.

IMPACT:

Given the importance of Rab GTPases in regulating critical cellular functions, it is not surprising that altered expression or mutation of Rab proteins and their interacting partners are associated with human disease. Rab25 and its binding partners are dysregulated in a number of tumour lineages. Functional studies demonstrate an impact of Rab25 on cell growth, proliferation, apoptosis, migration and invasion and *in vivo* tumourigenicity in mouse models, as well as an association with clinical outcomes. An understanding of the role of Rab25 in tumourigenesis will hasten the evolution of Rab25, its interacting partners and downstream targets as novel biomarkers and therapeutic targets.

associated gene expression signature, consisting primarily of genes involved in cellular metabolism, that predicts a poor outcome. Together, these data indicate that Rab25 induces resistance of cancer cells to nutrient stress, contributing to increased aggressiveness and poorer survival of patients with ovarian and breast cancer with high levels of Rab25, and identifies Rab25 as well as its functional consequences as potential therapeutic targets in tumours that express high levels of Rab25.

MATERIALS AND METHODS

Patient samples and cell culture

All patient samples and information were collected under IRB approved (LAB01-144) and HIPPA compliant protocols in MD Anderson Cancer Center. All patient samples contained greater than 80% tumour on histology. HEY, A2780 and SKOV3 ovarian cancer cells were maintained in RPMI 1640 containing 5% FBS. Immortalized ovarian surface epithelial cells IOSE29ht and IOSE80ht were maintained in MCDB105/M199 (50:50) containing 5% FBS as described previously (Cheng et al, 2004). ON-TARGET plus siRNAs specific to Rab25 and AKT were purchased from Dharmacon Inc. (Lafayette, CO). Rab25 shRNA was purchased from Origene (Rockville, MD).

Detection of autophagy

Autophagic vacuoles were detected by fluorescence microscopy labelled with LC3-GFP constructs. Fluorescent images were captured by fluorescence microscopy (Nikon Eclipse TE 2000-E, Germany) and analysed using the program IPLab (Scanalytic Inc). EM analysis of autophagy was carried out in High Resolution Electron Microscopy Facility at the MD Anderson Cancer Center core.

Detection of glucose uptake, cellular ATP levels, cellular glucose, glycogen and protein assays

Glucose uptake was measured by incubating cells with 2-H^3-deoxyglucose. Cellular ATP level was determined using an ATP Bioluminescence Assay Kit CLS II (Roche Applied Science, Indianapolis, IN) and normalized to cellular protein levels. Total cellular protein content was assessed using a BCA assay. Glucose and glycogen levels were assessed using glucose assay kit (Cat # K606-100) and glycogen assay kit (K646-100), respectively, obtained from BioVision Inc (Mountain View, CA) according to the manufacturer's protocol.

Cell death assays

Apoptotic cells were measured using paraformaldehyde fixed cells with an APO-DIRECT kit (Phoenix Flow Systems) with flow cytometry or the Cell Death Detection ELISA^{PLUS} (Roche Applied Science) according to the manufacturer protocol. Cell viability was detected using CellTiter-Blue® Cell Viability Assay (Promega, Madison, WI).

Protein expression profiling

WB analysis and reverse phase protein lysate array (RPPA) were carried as described previously (Cheng et al, 2004; Cheng et al, 2005).

Statistical analysis

Experiment results obtained were statistically evaluated by ANOVA or Student's *t*-test. Differences were considered significant for two-sided $p < 0.05$ or as designated. We estimated the survival probabilities

using the Kaplan–Meier method, and compared survival curves using the log-rank test. Statistical analysis was performed by GraphPad Prism V.4 (San Diego, CA) or SPSS 16.0 (Chicago, IL).

Author contributions

The overall study was conceived and designed by KWC, RA and GBM, with important contributions from SM, JSL, MC and JWG; KWC, RA, SM, MC performed the experiments; KWC, RA and JSL analysed the data; JSL and JWG contributed reagents or analysis tools; KWC, RA and GBM wrote the paper.

Acknowledgements

This work was supported by Breast SPORE Career Development Award and Department of Defense Breast Idea Award W81XWH-06-1-0488 to KWC, Cancer Research UK Clinician Scientist Fellowship C2757/A5902 to RA, National Institutes of Health SPORE (P50-CA83639) and PPG CA64602 to GBM and JWG, P30 grant CA16672-28 and Cancer Center Core Grant CA16672 and Ovarian Cancer Research Fund to GMB.

Supporting information is available at EMBO Molecular Medicine online.

The authors declare that they have no conflict of interest.

For more information

Rab25; Genecards:
http://www.genecards.org/cgi-bin/carddisp.pl?gene=RAB25

Gene expression analysis tool; BRB Array Tool:
http://linus.nci.nih.gov/BRB-ArrayTools.html

Gene Annotation Enrichment analysis; DAVID Bioinformatics Resources:
http://david.abcc.ncifcrf.gov/

Bioenergetics; Cellular Bioenergetics Forum:
http://www.seahorsebio.com/forum/index.php

Technology references:
Protein complementation Assay: PMCID: PMC1636760
Reverse phase protein array: PMID: 17041095, PMID: 17599930, PMID: 19102773, PMID: 19176552

References

Agarwal R, Jurisica I, Mills GB, Cheng KW (2009) The emerging role of the RAB25 small GTPase in cancer. Traffic 10: 1561-1568

Caswell PT, Spence HJ, Parsons M, White DP, Clark K, Cheng KW, Mills GB, Humphries MJ, Messent AJ, Anderson KI, *et al* (2007) Rab25 associates with alpha5beta1 integrin to promote invasive migration in 3D microenvironments. Dev Cell 13: 496-510

Chaudhury A, Howe PH (2009) The tale of transforming growth factor-beta (TGFbeta) signaling: a soigné enigma. IUBMB Life 61: 929-939

Cheng KW, Lahad JP, Kuo WL, Lapuk A, Yamada K, Auersperg N, Liu J, Smith-McCune K, Lu KH, Fishman D, *et al* (2004) The RAB25 small GTPase determines aggressiveness of ovarian and breast cancers. Nat Med 10: 1251-1256

Cheng KW, Lu Y, Mills GB (2005) Assay of Rab25 function in ovarian and breast cancers. Method Enzymol 402: 202-215

Cheng JM, Volk L, Janaki DK, Vyakaranam S, Ran S, Rao KA (2010) Tumor suppressor function of Rab25 in triple-negative breast cancer. Int J Cancer 126: 2799-2812

Colicelli J (2004) Human RAS superfamily proteins and related GTPases Sci STKE 2004: RE13

de Visser KE, Eichten A, Coussens LM (2006) Paradoxical roles of the immune system during cancer development. Nat Rev Cancer 6: 24-37

Degenhardt K, Mathew R, Beaudoin B, Bray K, Anderson D, Chen G, Mukherjee C, Shi Y, Gélinas C, Fan Y, *et al* (2006) Autophagy promotes tumor cell survival and restricts necrosis inflammation and tumorigenesis. Cancer Cell 10: 51-64

Edinger AL, Thompson CB (2002) Akt maintains cell size and survival by increasing mTOR-dependent nutrient uptake. Mol Biol Cell 13: 2276-2288

Eisenberg-Lerner A, Kimchi A (2009) The paradox of autophagy and its implication in cancer etiology and therapy. Apoptosis 14: 376-391

Elstrom RL, Bauer DE, Buzzai M, Karnauskas R, Harris MH, Plas DR, Zhuang H, Cinalli RM, Alavi A, Rudin CM, *et al* (2004) Akt stimulates aerobic glycolysis in cancer cells. Cancer Res 64: 3892-3899

Fan Y, Xin XY, Chen BL, Ma X (2006) Knockdown of RAB25 expression by RNAi inhibits growth of human epithelial ovarian cancer cells in vitro and *in vivo*. Pathology 38: 561-567

Fan Y, Dickman KG, Zong WX (2010) Akt and c-Myc differentially activate cellular metabolic programs and prime cells to bioenergetic inhibition. J Biol Chem 285: 7324-7333

Goldenring JR, Shen KR, Vaughan HD, Modlin IM (1993) Identification of a small GTP-binding protein, Rab25, expressed in the gastrointestinal mucosa, kidney, and lung. J Biol Chem 268: 18419-18422

Gottlob K, Majewski N, Kennedy S, Kandel E, Robey RB, Hay N (2001) Inhibition of early apoptotic events by Akt/PKB is dependent on the first committed step of glycolysis and mitochondrial hexokinase. Genes Dev 15: 1406-1418

Greenberg CC, Jurczak MJ, Danos AM, Brady MJ (2006) Glycogen branches out: new perspectives on the role of glycogen metabolism in the integration of metabolic pathways. Am J Physiol Endocrinol Metab 291: E1-E8

Gullino PM, Grantham FH, Courtney AH, Losonczy I (1967) Relationship between oxygen and glucose consumption by transplanted tumors *in vivo*. Cancer Res 27: 1041-1052

Hahn-Windgassen A, Nogueira V, Chen CC, Skeen JE, Sonenberg N, Hay N (2005) Akt activates the mammalian target of rapamycin by regulating cellular ATP level and AMPK activity. J Biol Chem 280: 32081-32089

Itzen A, Goody RS (2011) GTPases involved in vesicular trafficking: structures and mechanisms. Semin Cell Dev Biol 22: 48-56

Jin S, White E (2007) Role of autophagy in cancer: management of metabolic stress. Autophagy 3: 28-31

Kahn BB, Alquier T, Carling D, Hardie DG (2005) AMP-activated protein kinase: ancient energy gauge provides clues to modern understanding of metabolism. Cell Metab 1: 15-25

Karantza-Wadsworth V, Patel S, Kravchuk O, Chen G, Mathew R, Jin S, White E (2007) Autophagy mitigates metabolic stress and genome damage in mammary tumorigenesis. Genes Dev 21: 1621-1635

Kurtoglu M, Gao N, Shang J, Maher JC, Lehrman MA, Wangpaichitr M, Savaraj N, Lane AN, Lampidis TJ (2007) Under normoxia, 2-deoxy-D-glucose elicits cell death in select tumor types not by inhibition of glycolysis but by interfering with *N*-linked glycosylation. Mol Cancer Ther 6: 3049-3058

Lapierre LA, Caldwell CM, Higginbotham JN, Avant KM, Hall J, Beauchamp RD, Goldenring JR (2011) Transformation of rat intestinal epithelial cells by overexpression of Rab25 is microtubule dependent. Cytoskeleton 68: 97-111

Lee JS, Heo J, Libbrecht L, Chu IS, Kaposi-Novak P, Calvisi DF, Mikaelyan A, Roberts LR, Demetris AJ, Sun Z, *et al* (2006) A novel prognostic subtype of human hepatocellular carcinoma derived from hepatic progenitor cells. Nat Med 12: 410-416

Liang XH, Jackson S, Seaman M, Brown K, Kempkes B, Hibshoosh H, Levine B (1999) Induction of autophagy and inhibition of tumorigenesis by beclin 1. Nature 402: 672-676

Mathew R, Kongara S, Beaudoin B, Karp CM, Bray K, Degenhardt K, Chen G, Jin S, White E (2007) Autophagy suppresses tumor progression by limiting chromosomal instability. Genes Dev 21: 1367-1381

Meijer AJ, Codogno P (2004) Regulation and role of autophagy in mammalian cells. Int J Biochem Cell Biol 36: 2445-2462

Memmott RM, Dennis PA (2009) Akt-dependent and -independent mechanisms of mTOR regulation in cancer. Cell Signal 21: 656-664

Mizushima N (2004) Methods for monitoring autophagy. Int J Biochem Cell Biol 36: 2491-2502

Moreno-Sánchez R, Rodríguez-Enríquez S, Marín-Hernández A, Saavedra E (2007) Energy metabolism in tumor cells. FEBS J 274: 1393-1418

Mosesson Y, Mills GB, Yarden Y (2008) Derailed endocytosis: an emerging feature of cancer. Nat Rev Cancer 8: 835-850

Nam KT, Lee HJ, Smith JJ, Lapierre LA, Kamath VP, Chen X, Aronow BJ, Yeatman TJ, Bhartur SG, Calhoun BC, *et al* (2010) Loss of Rab25 promotes the development of intestinal neoplasia in mice and is associated with human colorectal adenocarcinomas. J Clin Invest 120: 840-849

Nevins JR, Potti A (2007) Mining gene expression profiles: expression signatures as cancer phenotypes. Nat Rev Genet 8: 601-609

Pelicano H, Martin DS, Xu RH, Huang P (2006) Glycolysis inhibition for anticancer treatment. Oncogene 25: 4633-4646

Pereira-Leal JB, Seabra MC (2000) The mammalian Rab family of small GTPases: definition of family and subfamily sequence motifs suggests a mechanism for functional specificity in the Ras superfamily. J Mol Biol 301: 1077-1087

Priebe A, Tan L, Wahl H, Kueck A, He G, Kwok R, Opipari A, Liu JR (2011) Glucose deprivation activates AMPK and induces cell death through modulation of Akt in ovarian cancer cells. Gynecol Oncol 122: 389-395

Proskuryakov SY, Konoplyannikov AG, Gabai VL (2003) Necrosis a specific form of programmed cell death? Exp Cell Res 283: 1-16

Ralser M, Wamelink MM, Struys EA, Joppich C, Krobitsch S, Jakobs C, Lehrach H (2008) A catabolic block does not sufficiently explain how 2-deoxy-D-glucose inhibits cell growth. Proc Natl Acad Sci USA 105: 17807-17811

Raynaud FI, Eccles S, Clarke PA, Hayes A, Nutley B, Alix S, Henley A, Di-Stefano F, Ahmad Z, Guillard S, *et al* (2007) Pharmacologic characterization of a potent inhibitor of class I phosphatidylinositide 3-kinases. Cancer Res 67: 5840-5850

Roach PJ (2002) Glycogen and its metabolism. Curr Mol Med 2: 101-120

Rudlowski C, Moser M, Becker AJ, Rath W, Buttner R, Schroder W, Schurmann A (2004) GLUT1 mRNA and protein expression in ovarian borderline tumors and cancer. Oncology 66: 404-410

Simons AL, Mattson DM, Dornfeld K, Spitz DR (2009) Glucose deprivation-induced metabolic oxidative stress and cancer therapy. J Cancer Res Ther 5: S2-S6

Tong X, Zhao F, Thompson CB (2009) The molecular determinants of de novo nucleotide biosynthesis in cancer cells. Curr Opin Genet Dev 19: 32-37

Tzaban S, Massol RH, Yen E, Hamman W, Frank SR, Lapierre LA, Hansen SH, Goldenring JR, Blumberg RS, Lencer WI (2009) The recycling and transcytotic pathways for IgG transport by FcRn are distinct and display an inherent polarity. J Cell Biol 185: 673-684

Vander Heiden MG, Cantley LC, Thompson CB (2009) Understanding the Warburg effect: the metabolic requirements of cell proliferation. Science 324: 1029-1033

Wangpaichitr M, Savaraj N, Maher J, Kurtoglu M, Lampidis TJ (2008) Intrinsically lower AKT, mammalian target of rapamycin, and hypoxia-inducible factor activity correlates with increased sensitivity to 2-deoxy-D-glucose under hypoxia in lung cancer cell lines. Mol Cancer Ther 7: 1506-1513

Watson RT, Kanzaki M, Pessin JE (2004) Regulated membrane trafficking of the insulin-responsive glucose transporter 4 in adipocytes. Endocr Rev 25: 177-204

Woodgett JR (1994) Regulation and functions of the glycogen synthase kinase-3 subfamily. Semin Cancer Biol 5: 269-275

Zhong D, Liu X, Schafer-Hales K, Marcus AI, Khuri FR, Sun SY, Zhou W (2008) 2-Deoxyglucose induces Akt phosphorylation via a mechanism independent of LKB1/AMP-activated protein kinase signaling activation or glycolysis inhibition. Mol Cancer Ther 7: 809-817

Zhong D, Xiong L, Liu T, Liu X, Liu X, Chen J, Sun SY, Khuri FR, Zong Y, Zhou Q, *et al* (2009) The glycolytic inhibitor 2-deoxyglucose activates multiple prosurvival pathways through IGF1R. J Biol Chem 284: 23225-23233

